X–RAY EMITTING EROS AS TRACERS OF BLACK HOLES-GALAXIES COEVOLUTION

M. Brusa[1], A. Comastri[2], E. Daddi[3], M. Mignoli[2], C. Vignali[4], G. Zamorani[2], F. Fiore[5], and L. Pozzetti[2]

[1]Max Planck Institut für Extraterrestrische Physik, Garching bei München, Germany
[2]INAF-Osservatorio Astronomico di Bologna, Bologna, Italy
[3]National Optical Astronomical Observatory, Tucson, USA
[4]Dipartimento di Astronomia, Università di Bologna, Bologna, Italy
[5]INAF-Osservatorio Astronomico di Roma, Monteporzio, Italy

ABSTRACT

The results from massive multiwavelength follow-up campaigns of X–ray sources discovered in both deep and shallow *Chandra* and XMM-*Newton* surveys have revealed a population of X-ray emitting Extremely Red Objects (X-EROs). We present the results obtained from the combined analysis of 80 ks XMM-Newton and 90 ks Chandra observations of a complete sample of optically selected EROs, with particular emphasys on the relationship between X-EROs and high luminosity, obscured quasars (QSO2). We also present several, independent findings indicating that a large fraction of X-EROs are hosted among the most massive galaxies at z=1-2, and thus can be used as lighthouses to investigate the link between the formation of massive ellipticals and the onset of AGN activity.

Key words: X–rays: surveys, galaxies: active, galaxies: Extremely Red Objects.

1. INTRODUCTION

Extremely Red Objects (EROs, R−K>5, Elston et al. 1988), initially detected in near–infrared ground–based imaging, have the colors expected for high-redshift passive ellipticals and have been used as tracers of distant (z> 1) and old spheroids. Reproducing their observational properties has probed to be extremely challenging for all current galaxy formation models. However, on the basis of a number of observational results, it has been pointed out that high-redshift passive ellipticals are only one of the various classes of extragalactic sources which make up the ERO population. Deep VLT spectroscopy from the $K20$ `survey` (Cimatti et al., 2002) has indeed shown that EROs are nearly equally populated by old, passively evolving systems and dusty star–forming galaxies over a similar range of redshift ($z = 0.8 - 2$ for both classes) and similar results are confirmed by both colour selection criteria (Mannucci et al., 2002) and by radio observations (Smail et al., 2002). A few individual objects have been also identified as high redshift (z=1–1.5) Active Galactic Nuclei (AGN) on the basis of the detection of strong emission lines in near–infrared and/or optical spectra (see e.g. Pierre et al. 2001).

A population of optically faint X–ray sources without any obvious AGN signature in the optical spectrum and with optical to near–infrared colors typical of high redshift ellipticals and starburst galaxies has been revealed in the deepest *Chandra* and XMM–*Newton* exposures (e.g. Hasinger et al. 2001; Barger et al. 2003; Szokoly et al. 2004). It has been suggested that the AGN population among EROs has the same X–ray properties of high–luminosity, highly obscured ($N_H > 10^{22}$ cm^{-2}) Type 2 Quasars (Mainieri et al., 2002; Alexander et al., 2002; Brusa, 2003). Further support for the result that a significant fraction of obscured AGN are hosted in EROs comes from near infrared observations of X–ray sources selected on the basis of their high X–ray to optical flux ratio (X/O> 10, Mignoli et al. 2004): the hosts of luminous, obscured hard X-ray sources with extreme X/O are among the most massive spheroids at z> 1.

The observed fraction of AGN among EROs can therefore help constraining models for the joint evolution of supermassive black holes and galaxies bulges (e.g. Granato et al. 2004; Merloni 2004; Marconi et al. 2005). Previous studies on the fraction of AGN among the EROs population, although having deep near–infrared and X–ray observations ($K \sim 21 - 22$ and the Megaseconds *Chandra* exposures) were limited in areal coverage (50–80 arcmin^2) and therefore were not suitable for detailed statistical analyses of the AGN EROs population.

We will briefly discuss how it is possible, combining near–infrared and X–ray data over a significantly larger area, to constrain the fraction of AGN EROs in near infrared selected samples and the masses of the black holes powering the X–ray emission in these sources.

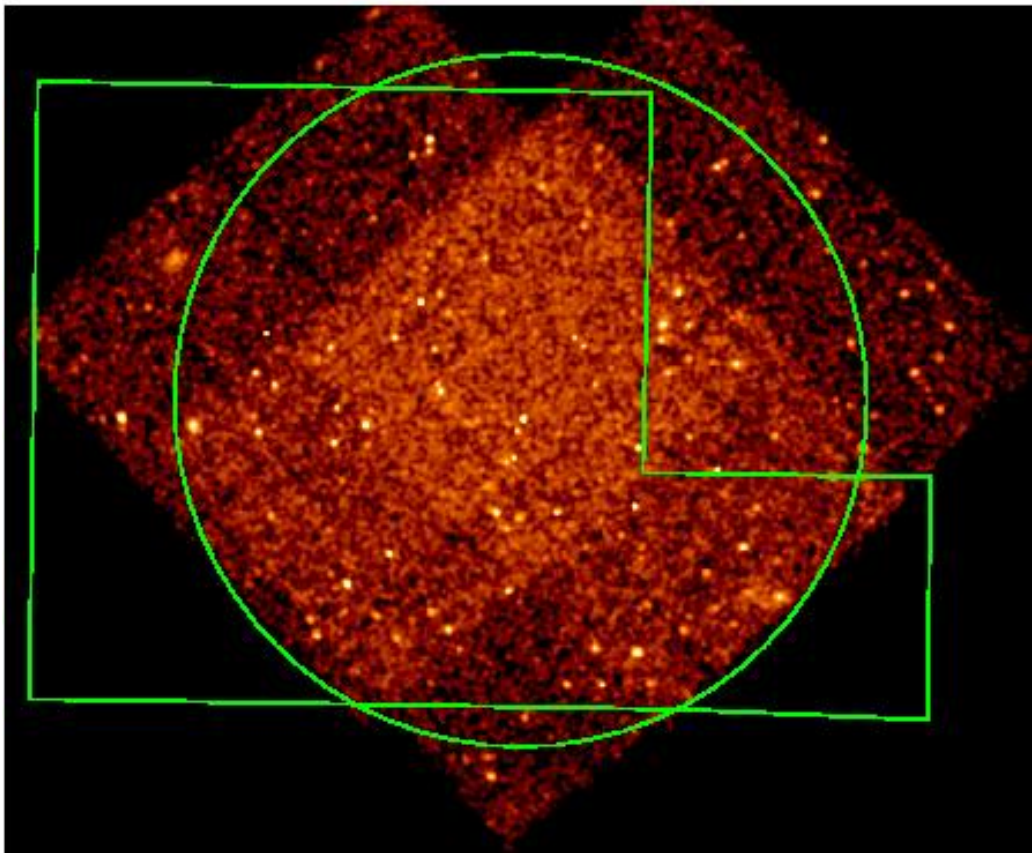

Figure 1. Chandra 0.5-8 keV image of the central region of the Daddi Field, with superimposed the 11 arcmin radius circle of the XMM-Newton analysis and the deepest region (~ 450 arcmin^2) covered with the K-band photometry (polygon). The X–ray image has been smoothed with a gaussian filter of 2 pixels. The central region (where the three pointings overlap) has an effective exposure time of ~ 85 ks.

2. THE XMM-NEWTON SURVEY OF EROS IN THE DADDI FIELD

2.1. X–ray data

We have started an extensive program of multiwavelength observations of the largest sample of near–infrared selected EROs available to date ($\sim$400 sources), selected over a contiguous field of ~ 700 arcmin^2 (the "Daddi field", Daddi et al. 2000). The sample is complete to a magnitude limit of Ks $\sim$19 and the field is covered by deep optical photometry in the R–band (R~ 26).
We have obtained with XMM–*Newton* a total of about 110 ks observing time, splitted in three different pointings (Brusa et al., 2005). The area analysed in the present work is ~ 380 arcmin^2 (see Fig. 1) and covers the region with a uniform coverage in the optical and near–infrared bands. The detection algorithm developed for the `Hellas2Xmm` survey (see Baldi et al. 2002 for details) was run on the 2–10 keV (hard band) cleaned events: 60 sources were detected down to a limiting flux of $S_{2-10} \sim 4 \times 10^{-15}$ erg cm^{-2} s^{-11}. The central (380 arcmin2) region of the Daddi Field has been subsequently imaged also by *Chandra*, with a mosaic of 3$\times$30 ks, partially overlapping observatios. Data were processed using version 3.2.1 of the CIAO software and mosaiced with the *merge_all* script. The full band (0.5-7 keV) *Chandra* mosaic is shown in Fig. 1.

[1]the count rate to flux conversion factor was derived assuming a power law with photon index Γ=1.7, absorbed by the Galactic column density in the direction of the field (N$_H$=5$\times$10^{20} cm^{-2}, Dickey & Lockman 1990), and weighted by the effective exposure times of the different EPIC cameras.

2.2. Optical identifications

At the faint X-ray and optical fluxes probed by the present survey the identification process of XMM sources is not straightforward due to the positional uncertainties associated with the XMM Point Spread Function. In order to identify the correct optical counterparts and to assess the statistical significance of the X-ray to optical associations we have used the "likelihood ratio technique" (Sutherland & Saunders, 1992). We were able to reliably identify ~ 80% of the X-ray sources, while for the remaining ~ 20% of the sources we were not able to provide an unambiguous association due to the faintness of the

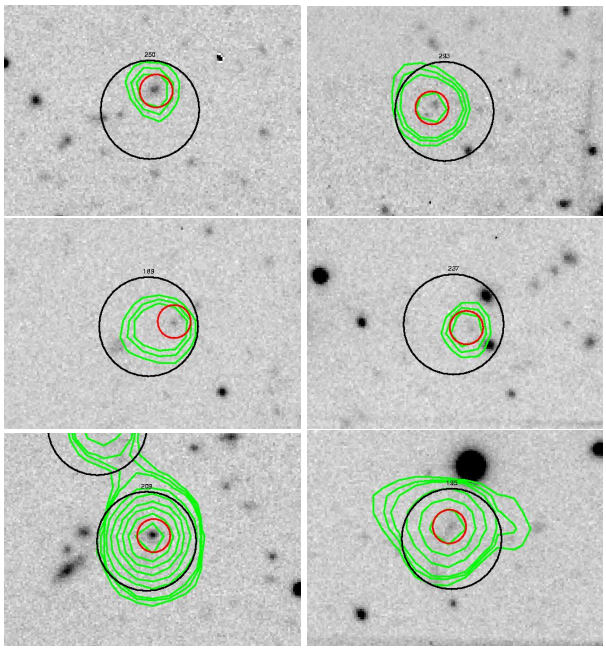

Figure 2. Finding charts in the R–band of 6 out of the nine X–ray emitting EROs in the Daddi Field. Large open circles (5″ radius) are centered on the XMM-Newton position; small red circles (1″ radius) mark the proposed EROs counterparts; green contours represent the Chandra sources.

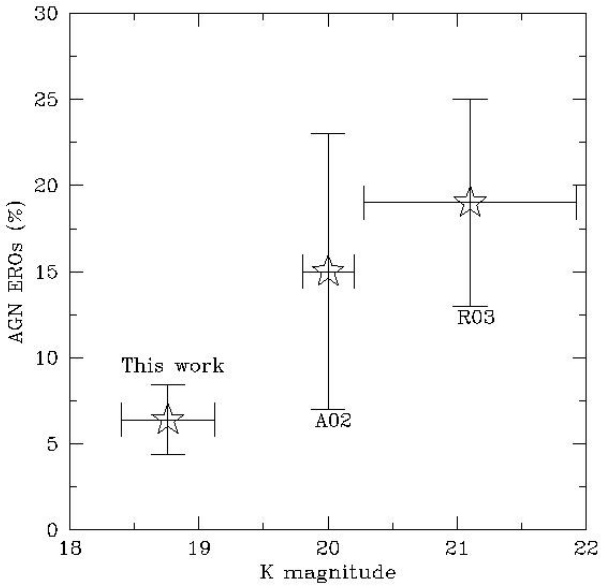

Figure 3. Fraction of AGN ERO as a function of the K–band magnitudes, as computed from three different samples: this work, the Alexander et al. sample (A02) and the Roche et al. sample (2003). The large errorbars associated with the A02 and R03 points are mostly due to the small area covered

possible counterparts (R>24) or to the presence of multiple sources, with similar likelihoods of being the correct identification, within the XMM error circles.
The XMM–*Newton* area analysed in this work includes 257 EROs: 173 EROs with Ks <18.8 over $\sim$ 380 arcmin^2, and 216 EROs with Ks <19.2 in the area in common with the deeper near–infrared coverage ($\sim$ 300 arcmin^2, see Fig. 1). Nine of the 257 EROs which fall within the XMM–*Newton* area are individually detected in the hard (2-10 keV) band. We checked our X–ray to EROs associations with the available *Chandra* data: all nine XMM–*Newton* detected EROs have been detected also by *Chandra* and in all the cases, thanks to the much sharper positional accuracy, the *Chandra* X–ray centroid points unambiguously to the candidate optical counterpart, further assessing the reliability of the adopted method for the identification of XMM–*Newton* sources. The finding charts of 6 X–ray emitting EROs in the R–band with superimposed the XMM-Newton error circle (5″) and the *Chandra* contours are shown in Fig. 2.

3. RESULTS FROM OUR SURVEY

In the XMM-*Newton* observation, the X–ray limiting flux corresponds to an X–ray luminosity $L_X \sim 10^{43}$ erg s^{-1} for z=1. Thus, the EROs X–ray emission is most likely powered by AGN activity, and the fraction of AGN among EROs in the present sample is *at least* $3.5 \pm 1.7\%$ (9/257). Conversely, the fraction of EROs among the hard X–ray population is much higher ($\sim$ 15%).
The fraction of X–ray detected EROs in K–selected samples has been reported by Alexander et al. (2002; hereinafter A02) and Roche, Almaini & Dunlop (2003; hereinafter R03) at different X–ray and K–band limiting fluxes. Combining the depth of the different samples with the observed X–ray to optical flux ratios distribution (see Next Section), it is possible to derive an estimate of the fraction of AGN EROs among K–selected samples as a function of the K–band magnitude only and independently from the X–ray limiting fluxes (see Brusa et al. 2005 for details). Figure 3 compares the fraction of AGN in our sample with those in the A02 and R03 samples and suggests that the fraction of AGN EROs among the K–selected EROs population is an increasing function of the K–band magnitude. The results from hard X–ray surveys indicate a space density of low–luminosity ($10^{42} - 10^{44}$ erg s^{-1}) AGN which is almost two orders of magnitudes higher than that of high luminosity sources (Fiore et al., 2003; Ueda et al., 2003). Thus, it is not surprising that the fraction of AGN EROs increases going toward faint fluxes (i.e., lower luminosities). It is worth remarking that the fraction of "active" objects in K–selected EROs samples can be used to constrain models which link the formation and evolution of galaxies and AGN (e.g. Merloni 2004).

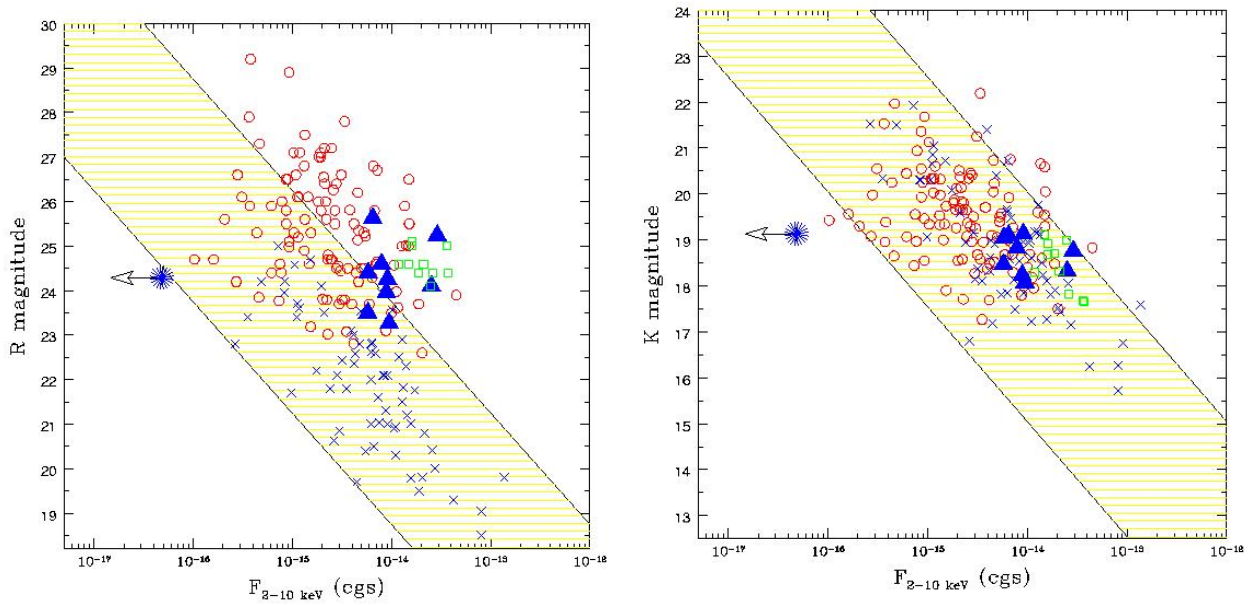

Figure 4. left panel: R–band magnitude vs. hard X–ray flux for EROs, serendipitously detected in hard X–ray surveys. Large filled triangles are the 9 hard X–ray selected EROs of this work; circles correspond to the EROs in the "literature sample"; squares are sources from the Hellas2Xmm *survey. As a comparison, BL AGN detected in the CDF–S and CDF–N surveys are also reported as crosses. The shaded area represents the region typically occupied by known AGN (e.g. quasars and Seyferts) along the correlation* $log(X/O) = 0 \pm 1$*. For comparison, we report the result of stacking analysis performed on the K20 EROs in the CDF–S field not individually detected in the Chandra observation (Brusa et al. 2002; upper limit at the faintest X–ray flux). Right panel: the same plot but in the K–band.*

4. X–RAY TO OPTICAL PROPERTIES

In order to investigate the nature of hard X–ray selected EROs and the link between faint hard X–ray sources and the ERO population, we have collected from the literature a sample of 128 X–ray detected EROs (including the 9 objects previously described). For about half of them (62/128) photometric or spectroscopic redshifts are available (data from: Mainieri et al. 2002; Barger et al. 2003; Willott et al. 2003; Brusa et al. 2005; Crawford et al. 2002; Szokoly et al. 2004; Mignoli et al. 2004). This sample is by no means homogeneous (e.g. the selection criteria for EROs are slightly different, R-K>5 or I-K>4 depending on the authors; or the K–coverage is not complete), but could be considered representative of EROs individually detected in the X–rays. The R–band magnitudes plotted versus the hard X–ray fluxes are reported in Fig. 4 (left panel): about half of the sources show an X–ray–to–optical flux ratio (X/O) larger than 10, shifted up by one order of magnitude from that of broad-line AGN, confirming independent results from near infrared observations of X–ray sources selected on the basis of their high X/O (e.g. Mignoli et al. 2004; Maiolino et al. 2005). On the contrary, when the X–ray to near–infrared properties are considered, all the X–ray detected EROs in the comparison sample occupy a locus which is indistinguishable from that occupied by unobscured QSO (Fig. 4, right panel). This result further corroborates the hypothesis that AGN EROs are obscured quasars.

5. X–RAY PROPERTIES OF AGN EROS

High obscuration in X–ray detected EROs is also revealed in the X–ray band, in agreement with the results from the optical band.
The average hardness ratio of the hard X–ray detected EROs in our XMM–*Newton* observation suggests substantial column densities at the source redshift. We have quantitatively estimated the intrinsic X–ray column densities for the 62 EROs in the comparison sample with a reliable spectroscopic or photometric identification. The results are reported in Fig. 5 (left panel). Almost all of the individually detected EROs have intrinsic $N_H > 10^{22}$ cm^{-2}, and they actually *are* heavily obscured AGN. This study confirms previous evidences mainly based on a Hardness Ratio analysis (A02) and on few isolated examples (e.g. Stevens et al. 2003; Severgnini et al. 2005), and unambiguously indicates that large columns of cold gas (even $> 10^{23}$ cm^{-2}) are the rule rather than the exception among X–ray bright EROs.

5.1. EROs and QSO2: a selection criterion

Given the high–redshift (z>0.8) and the average X–ray flux ($\sim 4\times10^{-15}$ erg cm^{-2} s^{-1}) of these objects, it is not surprising that the majority of X–ray detected EROs have high X–ray luminosities ($L_X > 10^{43}$ erg s^{-1}). Moreover, according to our analysis, a significant fraction of them have X–ray luminosities exceeding 10^{44} erg s^{-1},

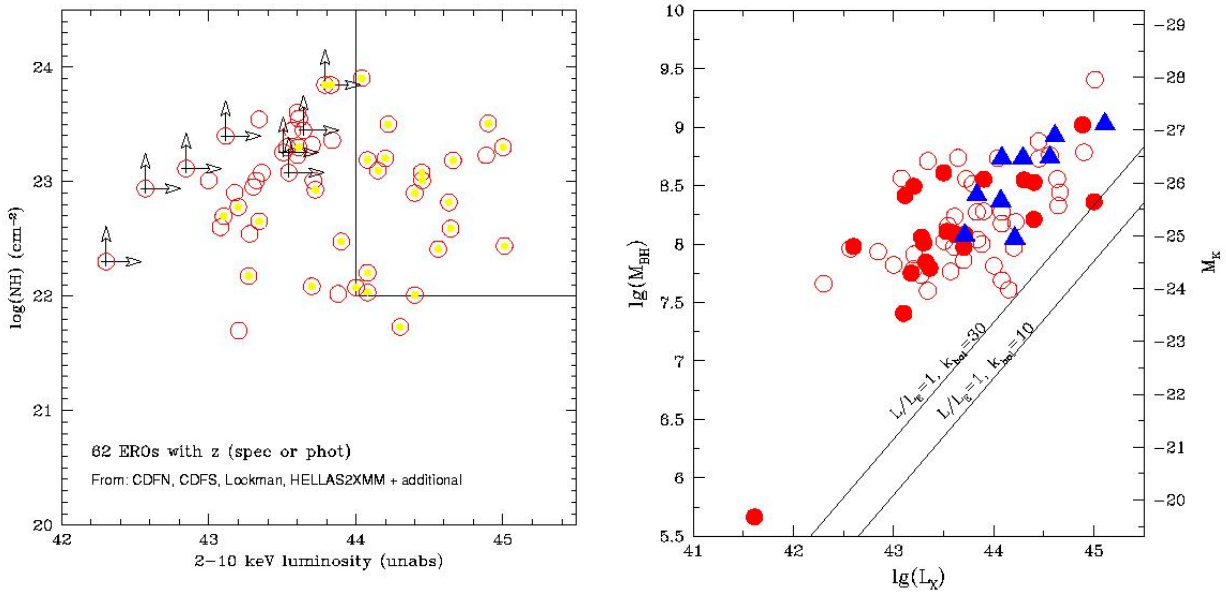

Figure 5. Left panel: Logarithm of the absorbing column density (N_H) versus the logarithm of the unabsorbed X–ray luminosity in the 2-10 keV band for all the X–ray detected EROs with spectroscopic or photometric redshifts from the literature sample. Filled symbols are those with X/O $>$ 10 (see text). In the upper right corner the "QSO2 locus" is highlighted. Right panel: The M_{BH} obtained applying the Marconi & Hunt (2003) relation for the identified EROs versus the L_X. Symbols as in Fig. 4. Filled circles are sources with spectroscopic redshift. The continuous lines represent the expected correlation between the two plotted quantities for two different assumptions on the bolometric correction and $L_{\rm bol}/L_{\rm E}$=1.

and therefore lie within the quasar regime (see also Severgnini et al. 2005, and this volume). The large intrinsic column densities further imply that AGN EROs, selected at bright X–ray fluxes, have properties similar to those of QSO2, the high–luminosity, high–redshift Type 2 AGNs required by X–Ray Background synthesis models (Comastri et al., 2001; Gilli et al., 2001). Among the X–ray detected EROs, the higher is the luminosity, the higher is the X–ray to optical flux ratio (filled symbols in left panel of Fig. 5). This confirms that a selection based on X/O $>$ 10 is a powerful tool to detect high–luminosity, highly obscured sources (see Fiore et al. 2003) and it is even stronger when coupled with a previous selection on the extremely red colors. Given that the search for QSO2 on the basis of detection of narrow optical emission lines is extremely time consuming and als already challenging the capabilities of the largest optical telescopes, all the findings discussed above support the idea that hard X–ray surveys coupled with near–infrared observations provide an efficient method in detecting QSO2.

5.2. The masses and level of activity of X-ray emitting EROs

Indipendent arguments suggest that the near–infrared emission of X–ray selected *obscured* AGN is dominated by their host galaxy starlight (see e.g. Mainieri et al. 2002; Mignoli et al. 2004). Using the correlation between the bulge K–band luminosity and the BH mass published by Marconi & Hunt (2003), it is possible to estimate the masses of the obscured SMBH powering the X–ray emission of the 62 EROs with redshift information in the literature sample and the 9 EROs of the present work for which redshifts and luminosities have been estimated from the Fiore et al. (2003) relation. The BH masses have been computed assuming that 1) the measured K band light is completely due to the bulge component and therefore the AGN emission does not significantly contribute to the near-IR light and that 2) the shape of the Marconi & Hunt (2003) relation does not significantly evolve with redshift and/or luminosity.
The M_{BH} obtained through a chain of assumptions and neglecting the uncertainties associated to the observed relations, are plotted versus the L_X in the right panel of Fig. 5. We note that the presence of a disk or a residual point–source contribution would lower the bulge luminosity and in turn the mass determination, that can therefore be considered as conservative upper limits.
The absorption corrected X–ray luminosity can be translated into a bolometric luminosity assuming a bolometric correction factor ($L_{bol} = k_{bol} \times L_X$)[2]. The continuous lines in the right panel of Fig. 5 represent the relation between the BH mass and the X–ray luminosity in the hypothesis of Eddington limit accretion ($L_{bol}/L_{edd} = 1$) and for two different values (k_{bol}=10 and k_{bol}=30) of the

[2]A robust estimate for the bolometric correction ($k_{bol} \sim 30$) is available only for bright unobscured quasars (Elvis et al., 1994); lower values ($k_{bol} \sim 10$–20) appear to better reproduce the observed spectral energy distribution of Seyfert like galaxies (Fabian, 2004) and of a few heavily obscured, luminous sources (Comastri, 2004).

bolometric correction. Despite the large scatter observed in Fig. 5 – for a given BH mass the corresponding luminosity ranges up to 2 orders of magnitudes – there is a clear trend between the X–ray luminosity and the BH mass; the dispersion can be reasonably well explained by a spread in the Eddington ratios in the range L_{bol}/L_{edd}=10^{-3}–10^{0}, most of the sources having $L_{bol}/L_{edd} > 10^{-2}$. Both the BH masses and the Eddington ratios derived above are consistent with a scenario in which X–ray detected EROs are obscured quasars emitting in a radiatively efficient way, in agreement with the results of Merloni (2004) and McLure & Dunlop (2004)).

REFERENCES

Alexander, D.M., Vignali, C., Bauer, F.E., et al. 2002, AJ 123, 1149 (A02)

Baldi, A., Molendi, S., Comastri, A., et al. 2002, ApJ, 564, 190

Barger, A.J., Cowie, L. L., Capak, P., et al. 2003, AJ, 126, 632

Brusa, M., Comastri, A., Daddi, E., Cimatti, A., Mignoli, M., & Pozzetti, L. 2002, ApJ, 581, L89

Brusa, M. 2003, AN, 324, 116;

Brusa, M., Comastri, A., Daddi, E., et al. 2005, A&A, 432, 69

Cimatti, A., Daddi, E., Mignoli, M., et al. 2002, A&A 381, L68

Comastri, A., Fiore, F., Vignali, C., et al. 2001, MNRAS, 327, 781

Comastri, A., 2004, in “Supermassive Black Holes in the Distant Universe”, Ed. A. J. Barger. Kluwer Academic Publishers, Chapter 8

Crawford, C.S., Gandhi, P., Fabian, A.C., et al. 2002, MNRAS, 333, 809

Daddi, E., Cimatti, A., Pozzetti, L., et al. 2000, A&A, 361, 535

Dickey, J.M., & Lockman, F.J. 1990 ARA&A, 28, 215

Elston, R., Rieke, G.H., & Rieke, M.J., 1988, ApJ 331, L77

Elvis, M., Wilkes, B.J., McDowell, J.C., et al. 1994, ApJS, 95, 1

Fabian, A.C., 2004, in ”Coevolution of Black Holes and Galaxies”, Carnegie Observatories Astrophysics Series, Vol. 1, pag. 447, ed. L.C. Ho (Cambridge Univ. Press), astro-ph/0304122

Fiore, F., Brusa, M., Cocchia, F. et al. 2003, A&A, 409, 79

Gilli, R., Salvati, M., & Hasinger, G. 2001, A&A, 366, 407

Granato, G.L., De Zotti, G., Silva, L., Bressan, A. & Danese, L., 2004, ApJ, 600, 580

Hasinger, G., Altieri, B., Arnaud, M., et al. 2001, A&A, 365, L45

Mainieri, V., Bergeron, J., Hasinger, G., et al. 2002, A&A, 393, 425

Maiolino, R., Mignoli, M., Pozzetti, L., et al. 2005, A&A, in press, astro-ph/0509244

Mannucci, F., Pozzetti, L., Thompson, D., et al. 2002, MNRAS 329, L57

Marconi, A., & Hunt, L., 2003, ApJ, 589, L21

Marconi, A., Risaliti, G., Gilli, R., Hunt, L.K., Maiolino, R., Salvati, M., 2005, MNRAS, 351, 169

McLure, R.J., & Dunlop. J.S., 2004, to appear in the proceedings of “Multiwavelength AGN Surveys”, astro–ph/0405393

Merloni, A., 2004, MNRAS, 353, 1035

Mignoli, M., Pozzetti, L., Comastri, A., et al. 2004, A&A, 418, 827

Pierre M., et al., 2001, A&A 372, L45

Roche, N., Dunlop, J., & Almaini, O. 2003, MNRAS, 346, 803 (R03)

Severgnini, P., Della Ceca, R., Braito, V. et al. 2005, A&A, 431, 32

Severgnini, P., Della Ceca, R., Braito, V. et al. 2006, this volume

Smail, I., Owen, F.N., Morrison, G.E. et al. 2002, ApJ, 581, 844

Stevens, J.A., Page, M.J., Ivison, R.J., et al. 2003, MNRAS, 342, 249

Sutherland, W. & Saunders, W. 1992, MNRAS, 259, 413

Szokoly, G.P., Bergeron, J., Hasinger, G. et al. 2004, ApJS, check refe

Ueda, Y., Akiyama, M., Ohta, K., & Miyaji, T., 2003, ApJ, 598, 886

Willott, C., Rawlings, S., Jarvis, M.J., Blundell, K.M. 2003, MNRAS, 339, 397